IChemE

0263–8762/01/$10.00+0.00

Trans IChemE, Vol. 79, Part A, January 2001

THE TRANSIENT RESPONSE OF GRANULAR FLOWS IN AN INCLINED ROTATING CYLINDER

R. J. SPURLING, J. F. DAVIDSON and D. M. SCOTT

Department of Chemical Engineering, University of Cambridge, Cambridge, UK

This paper reports the results of an experimental and theoretical study to investigate the transient response of the granular flow through a laboratory scale inclined rotating cylinder to large step changes in one of three variables: (i) mass feed rate, (ii) rotation speed or (iii) axis inclination. Experimental measurements are reported for a range of operating conditions, sizes of step and a number of cylinder geometries. A mechanistic model for the transient response is derived based on a published steady state model. The dynamic model parameters are the cylinder radius, length, discharge dam height, axis inclination and rotation speed, the granular feed rate, and the bulk density and dynamic angle of repose of the granular material. The model has no adjustable parameters, making it useful for scale-up. The model takes the form of a non-linear partial differential equation, equivalent to a one dimensional unsteady diffusion equation with variable coefficients, and solution has been obtained numerically.

Good agreement is found between the model and experiment both in the range of cases considered in the current study, and also for published experimental work, for which the cylinder size and granular material properties differ substantially from those of this work.

Keywords: rotary kilns; granular flow; transients; control.

INTRODUCTION

Rotary kilns play an important role in the processing of granular materials in the chemical and metallurgical industries in which they are used in operations such as mixing, drying, heating and gas-solid reactions. In general, processes are endothermic, require long residence times, and are controlled by heat addition and the exchange of gaseous reagents and products from within the solid phase. Example processes include calcination, pyrolysis and sintering.

Here cylindrical kilns without lifters are described. Driers often have lifters, but these are outside the scope of this paper.

The kiln typically consists of a refractory lined steel cylinder of diameter 2-3 m with a ratio of length to diameter greater than 20. The kiln is partially filled with granular material to a level generally less than 30% by volume. The kiln is inclined along its length at an angle to the horizontal of a few degrees and slowly rotated about its axis at a rotation speed, n, of 1 rev per 5–10 minutes. In the continuous mode, the granular material is fed to the upper end of the kiln and forms a continuously circulating, well-mixed bed resting against the kiln wall. The granular bed is slowly conveyed along the kiln length as a result of the continuous circulation and the force of gravity down the slope. Furnace gases and gaseous reagents are passed through the kiln above the granular bed, and mass and heat transfer occurs through the bed surface and between the kiln wall and that part of the granular bed in contact with it.

In order to understand the processes taking place in the kiln, it is necessary to understand the solids motion, as this interacts with processes such as heat and mass transfer, and reaction. To this end, investigation of the granular flow aims to elucidate the relationship between the operating parameters, kiln geometry and granular material properties, and three principal features of the system:

(i) the bulk motion of the granular bed characterized by the hold-up profile, mean residence time and residence time distribution,
(ii) the radial mixing and segregation of solids as a result of particle size, shape and density differences, and
(iii) the regimes of transverse solids motion.

The transverse motion of a bed of granular material in a rotating drum is categorized by Henein *et al.*[1] as a function of Froude number given by $(2\pi n)^2 R/g$, where R is the kiln radius and g the acceleration of gravity. As n is increased, three categories of behaviour are observed within the range of low and moderate Froude numbers applicable to kiln operation: at low speeds, slipping may occur in which the granular bed remains at rest and the bed slips at the drum wall. With further increase of n there is slumping, in which the granular bed is continuously lifted up by the drum wall and periodically falls down the surface in discrete avalanches. The period between slumps falls with increased rotation speed, eventually leading to the rolling mode in which there is a thin surface layer of continuously falling particles forming a plane free surface. To ensure good transverse mixing, rotary kilns are generally operated in the slumping or rolling regimes. The analysis given here relates to the slumping or rolling regimes, i.e. low kiln rotation speeds, when centrifuging forces are negligible. In the

experiments reported, the Froude number is between 2×10^{-4} and 2.5×10^{-3}.

The bulk motion of the granular bed in steady state operation has been investigated experimentally by a number of authors in laboratory and pilot scale devices[2–9]. Modelling of the solids motion observed is principally of two types: empirical correlations in terms of dimensionless parameters[10], and mechanistic models, as first proposed by Saeman[11], and Kramers and Croockewit[2]. The latter approach proposes a mechanism for the granular flow through the kiln based on a simple average particle motion determined by the dynamic angle of repose and bulk density of the granular material. Generally good qualitative agreement and reasonable quantitative correlation is found between the experimental results and the model.

A number of industrial situations give rise to transient behaviour in the solids motion, such as start-up, irregularities in the granular feed rate and fluctuations in the feed material properties. In order to devise an effective control strategy, and successful process models, it is therefore important to understand the unsteady solids motion resulting from sudden changes in the operating variables, namely the rotation speed, the solids feed rate and slope of the kiln axis.

There is little published work dealing with the dynamic case. A small set of experimental measurements of the variation in the discharge rate of solids with time following step changes in the operating conditions is reported by Sai *et al.*[12] and Sriram and Sai[13], and compared to the predictions of a non-linear model formulated as a multi-step algorithm proposed by Perron and Bui[14]. Reasonable agreement is observed for step changes in the feed rate and rotation speed, though the model fails to predict an initial lag observed in the response, and fails when two or more variables are changed simultaneously.

This paper reports an experimental investigation of the bulk motion of a sand bed in a laboratory scale cylinder immediately after a step disturbance in one of the operating variables. Experimental measurements are reported of the discharge flow rate and bed hold-up profile during the transient response for a range of operating conditions, different kiln geometries and different sizes of step up and step down in the disturbance variable. A mechanistic model is derived for the unsteady state case with no fitted parameters. Excellent quantitative agreement is found between the model and the experimental results.

EXPERIMENTAL WORK

Description of Apparatus

The apparatus consisted of a clear Perspex cylinder of length 1 m and internal radius 0.0515 m lined on the inner wall with sandpaper of particle size 127 μm. The cylinder was supported by four rubber rollers and rotated by an electric motor and belt drive up to a maximum rotational speed of 0.125 r.p.s., giving a rotational Froude number of 0.0036. The cylinder mounting was hinged so that the feed end could be raised above the discharge end and the cylinder axis inclined at an angle of 0°–5° to the horizontal. The feed end was fitted with a thin dam of height 0.029 m to prevent back spillage of the feed; this height was measured radially from the cylinder wall. At the discharge end there was either no dam or a thin dam of height 0.0105 m. Granular material was fed through a conical feed hopper from a COOTE FVC 9 vibratory feeder unit with digital control. An independent set of experiments verified that the mass flow rate at a given controller setting was constant and repeatable. Outflow of material at the discharge end was directed into a collection bucket on top of an electronic balance, maximum load 4 kg and resolution $\pm$ 0.05 g. The balance was connected to a PC and the reading logged at a constant frequency up to a maximum of once per second. An average mass flow rate was obtained by calculating the change in mass over a short time interval: for time intervals less than that for one cylinder rotation, the mass flow rate contained periodic oscillations of the same frequency as the rotation; to eliminate this effect, the time intervals used were greater than or equal to the time taken for two cylinder rotations.

A number of experiments were performed on an equivalent piece of apparatus at the Department of Chemical Engineering, University of Birmingham, as described by des Boscs[15]. The cylinder used was of length 1 m and internal radius 0.119 m.

Experiments were performed with sieved sand of particle size range 300–600 μm and mean particle size 490 μm. The poured bulk density was measured in a 500 ml volume and found to be 1600 kg m^{-3}. The static angle of repose was measured near the centre of the experimental cylinder following rotation with the axis horizontal; it was found to be $32^\circ\pm 0.5^\circ$. In the analysis that follows it is assumed the static and dynamic angles of repose are equal: in fact they differ by a few degrees, but this difference is not important for the theory. For the experimental parameters considered, the bed was in the rolling mode, as described by Henein *et al.*[1].

Experimental Method

Experiments were performed to measure the transient response of the discharge mass flow rate following a step change in the feed flow rate. The effect of the initial flow rate, magnitude and direction of the step, axis inclination, rotation speed and discharge dam height on the response were considered. The apparatus was set up with the desired parameter values and then the granular feed and the cylinder rotation were started. The apparatus was operated at a constant feed rate and rotation speed until the discharge mass flow rate became constant and equal to the feed rate. The granular feed and the cylinder rotation were then stopped and the granular feed setting changed. The granular feed and cylinder rotation were restarted simultaneously, the granular feed with a new value and the rotation speed with the same value as before stopping. The apparatus was operated at the new feed rate until the discharge mass flow rate reached the same steady value as the feed. Similar experiments were performed with step changes in the rotation speed and axis inclination with all other parameters held constant.

A second set of experiments was performed to measure the development of the axial bed depth profile in the cylinder during the transient response. Experiments were performed as previously, but at a number of times following the step, the granular feed and cylinder rotation were stopped, halting motion in the bed. The bed depth was measured, as described below, and then the material feed

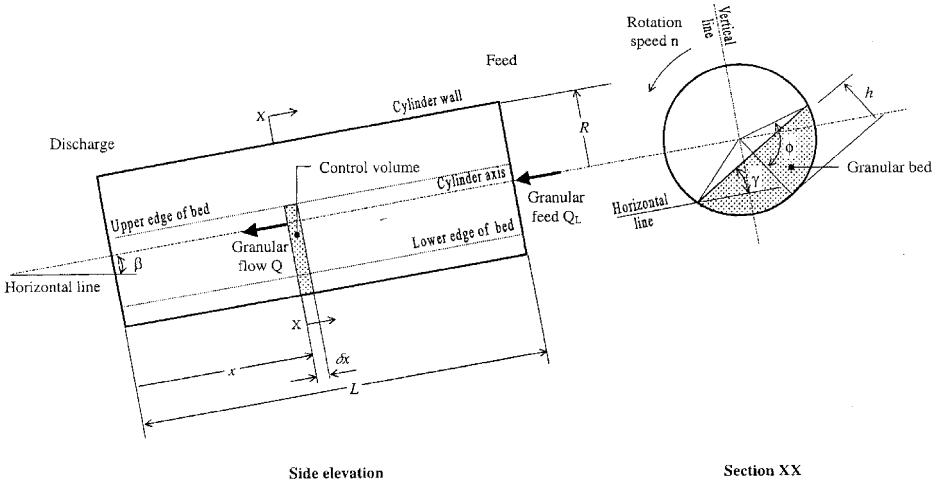

Figure 1. Schematic diagram of granular material transport through an inclined and slowly rotated cylinder.

and cylinder rotation restarted simultaneously. It was verified that stopping and starting the cylinder operation did not change the response by comparing the discharge flow rate obtained using this method with the results from an identical continuous experiment: the two cases were found to be equivalent.

In order to measure the bed depth, the sandpaper lining of the inner wall was split into a series of 23 mm axial sections separated by clear gaps of 2 mm. A millimetre scale was marked around the circumference at the edge of each gap. With the rotation and feed stopped, a lamp was used to illuminate the inside of the cylinder and the relative angular position of the upper and lower edges of the bed measured by observation through the wall. The bed depth was calculated by assuming the bed surface formed a straight line between the upper and lower edges of the bed. A measurement error of ± 0.75 mm was estimated in each reading and the resultant error in the bed depth calculated. It was verified that the experimental measurements were repeatable within the measurement error range by comparison of five independent sets of measurements of the same steady state bed depth profile.

THEORY

A dynamic model for the time dependent flow in an inclined rotating cylinder, subject to a disturbance in the feed rate, rotation speed, or axis inclination, is derived by combining a steady state model and material balance.

Steady State Model

A steady state model for the transport of granular material through an inclined slowly rotated cylinder was first derived by Saeman[11], and Kramers and Croockewit[2]. A schematic representation of the cylinder and details of notation are given in Figure 1. The model proposes that the mechanism of granular flow through the cylinder consists of a simple average particle motion, shown schematically in Figure 2. It is proposed that in a cross-section of the bed perpendicular to the cylinder axis there are two regions with distinct modes of particle behaviour:

- On the bed surface there is a thin layer of particles falling under gravity from the upper to the lower half of the bed. Transport through the cylinder occurs by the component of this motion parallel to the cylinder axis.
- Beneath the surface layer the granular bed rotates as a rigid body about the cylinder axis. Each particle is assumed to be transported along a circular track from the lower to the upper half of the bed where it re-enters the falling layer.

It is assumed that:

- On average the trajectory of a particle in the falling layer is straight and inclined to the horizontal plane at the dynamic angle of repose of the bed material.
- For the range of cylinder rotation speeds considered, the granular material dynamic angle of repose is constant and equal to the static angle of repose.

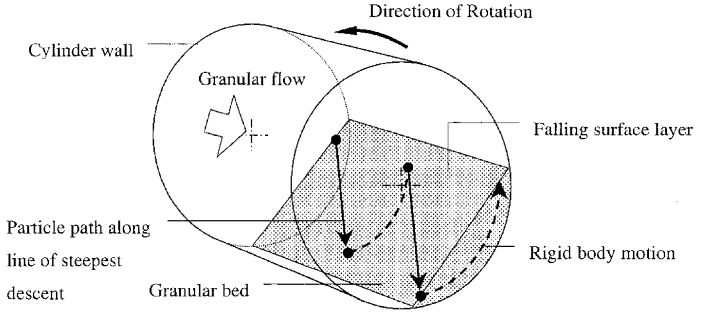

Figure 2. Schematic diagram of particle motion in the granular bed.

- There is no slip between the cylinder wall and the granular bed: thus, apart from the falling surface layer, it is assumed that the granular bed rotates about the cylinder axis in solid body motion at the same angular velocity as the cylinder.
- The residence time of particles in the falling layer is negligible in comparison with that in the rigid body region. This implies that the mean particle velocity in the falling layer is significantly greater than that in the bulk. By continuity, the thickness of the active layer is very small in comparison to the total depth of the bed.
- The depth of the granular bed at the cylinder discharge end is equal to the height of the discharge dam.

Henein *et al.*[1] and des Boscs[15] describe the results of experimental studies of the relationship between the dynamic angle of repose in a rolling bed and the cylinder rotation speed, bed depth and cylinder diameter. The dynamic angle of repose was found to be independent of the rotation speed and bed depth, and to decrease with increasing drum diameter.

Experimental measurement of the falling layer residence time was made by Lebas *et al.*[3], who found that the fraction of the total residence time spent in the falling layer is independent of the cylinder rotation speed and increases as the bed depth decreases. Experimental measurements of the active layer thickness in the rolling mode of bed behaviour were made by Boateng *et al.*[16], Henein *et al.*[1], Nakagawa *et al.*[17] and Parker *et al.*[18]. The material type, the rotation speed and the fill level were found to be important. The thickness of the falling layer as a fraction of the bed depth was found to be between 10% and 40%; it increased with rotation speed, decreased with increasing bed depth and decreased with particle size.

In the first stage of the model formulation, the particle path geometry is analysed to obtain a general expression for the distance travelled along the cylinder axis as a result of a single fall down the bed surface, see Appendix. To simplify the geometric analysis it is assumed that the slope of the bed surface relative to the cylinder axis, $\mathrm{d}h/\mathrm{d}x$, and the slope of the axis, β, are small. By neglecting the falling layer residence time, the time taken for the particle to complete a single circulation can be derived from the bed geometry. The circulation time and axial distance of travel are then combined to produce a general expression for the mean axial velocity of a particle. The analysis of individual particle motion is then integrated over a cross-section of the bed perpendicular to the cylinder axis. The result, see Appendix, is the following expression for the volumetric flow rate, Q, through the cross-section which is dependent on: the cylinder radius, R, axis inclination, β, rotation speed, n, and the dynamic angle of repose, γ, of the bed material.

$$Q = \frac{R^3 \sin^3 \phi}{C_A}\left\{R \sin \phi \frac{\mathrm{d}\phi}{\mathrm{d}x} + C_B\right\} \tag{1}$$

Equation (1) is essentially the same as the result originally given by Saeman[11], and by Kramers and Croockewit[2]. The angle ϕ, giving a measure of bed depth, is shown in Figure 1; x is the axial distance, measured from the discharge end. The coefficients C_A and C_B are defined as:

$$C_A = 3 \tan \gamma / 4\pi n \tag{2}$$

$$C_B = \tan \beta / \cos \gamma \tag{3}$$

Rearranging (1) gives a non-linear first order ordinary differential equation (ODE) with constant coefficients:

$$\frac{\mathrm{d}\phi}{\mathrm{d}x} = \frac{C_A Q}{R^4 \sin^4 \phi} - \frac{C_B}{R \sin \phi} \tag{4}$$

The single boundary condition required for solution is obtained from the assumption that the bed depth at the cylinder discharge end is equal to the height of the discharge dam:

$$\phi[x = 0] = \phi_0 \tag{5}$$

The height of the dam is $h_0 = R(1 - \cos \phi_0)$. This boundary condition becomes inappropriate in the case of no dam, when $\phi_0 = 0$. Substitution of this boundary value into (4) gives $\left(\frac{\mathrm{d}\phi}{\mathrm{d}x}\right)_{x=0} \rightarrow \infty$, a non-physical singularity that is inconsistent with the small angle assumptions made in the analysis of the particle path. In the case of no dam, it is therefore assumed that the discharge bed depth has a small value. The solution for the bed depth is found to be insensitive to the small value taken and in the calculations reported it has been assumed the bed depth is equal to the mean particle size.

Equation (4) is integrated numerically from the discharge end up to the feed end to calculate the axial bed depth profile, and hence from the geometry of the bed, the hold-up profile. The hold-up profile is integrated along the length of the cylinder to calulate the total inventory, and then divided by the volumetric flow rate to give the mean particle residence time.

A number of authors have performed experimental studies to identify the effect of process parameters on the steady state granular flow through laboratory scale inclined rotating cylinders. Measurement of the total hold-up is reported by Kramers and Croockewit[2], and Vahl and Kingma[4]. Measurements of the axial bed depth or hold-up profile are reported by Abouzeid and Fuerstenau[5], Chaterjee *et al.*[6,7], des Boscs[15], Hogg *et al.*[8], Lebas *et al.*[3] and Sai *et al.*[9]. These authors conclude there is good correlation between the experimental results and values calculated from the model. A number of authors quantify the level of correlation:

- Kramers and Croockewit[2] describe a systematic deviation in the calculated total hold-up with a mean square error of 15% compared to an experimental accuracy of $\pm 5\%$; for low loadings the calculated value is too low, for high loadings too high.
- des Boscs[15] finds differences of less than 5% between the experimental and calculated bed depth.

As a result of this body of experimental evidence validating the steady state model, it was decided to adopt the same form of model for the time dependent case.

Dynamic Model

In formulating a model for the unsteady case, it is assumed that the time scale of dynamic effects is large compared to the time of a particle flight in the falling layer. It follows that local to an axial element of length δx the axioms of the steady state model remain valid. Hence, each element can be treated as being in quasi-steady-state and so equation (4) can be taken as the basis of the unsteady state analysis.

In the dynamic case there are two dependent variables, the bed geometry and the local volumetric flow rate, which are functions of two independent variables, the axial position, x, and time, t. The ODE given in (4) is rewritten to give a first order partial differential equation (PDE) in terms of these variables:

$$\left(\frac{\partial\phi}{\partial x}\right)_t = \frac{C_A Q}{R^4 \sin^4\phi} - \frac{C_B}{R\sin\phi} \tag{6}$$

A second first order PDE is required: to obtain this, a dynamic volume balance over a differential axial control volume is considered, as shown in Figure 1. This gives the following relation between the bed area in a transverse cross-section, A, and the volumetric flow rate through the cross-section:

$$\left(\frac{\partial A}{\partial t}\right)_x = \left(\frac{\partial Q}{\partial x}\right)_t \tag{7}$$

Here it has been assumed that A, Q and ϕ are continuous functions of x, even though each element δx is finite, as explained in the Appendix; but $\delta x \ll L$, the length of the cylinder. From the geometry, the bed area can then be expressed in terms of ϕ:

$$A = R^2(\phi - \sin\phi\cos\phi) \tag{8}$$

Differentiating this expression with respect to time gives:

$$\left(\frac{\partial A}{\partial t}\right)_x = 2R^2\sin^2\phi\left(\frac{\partial\phi}{\partial t}\right)_x \tag{9}$$

When combined with (7), this gives the required second first order PDE:

$$\left(\frac{\partial Q}{\partial x}\right)_t = 2R^2\sin^2\phi\left(\frac{\partial\phi}{\partial t}\right)_x \tag{10}$$

The pair of first order PDEs given by equations (6) and (10) can be reformulated in terms of the single dependent variable ϕ. Differentiating (6) with respect to x and then eliminating Q by substitution from (10) gives the following non-linear second order PDE:

$$2R^2\sin^2\phi\left(\frac{\partial\phi}{\partial t}\right)_x = \frac{\partial}{\partial x}\left\{\frac{R^3\sin^3\phi}{C_A}\left\{R\sin\phi\left(\frac{\partial\phi}{\partial x}\right)_t + C_B\right\}\right\}_t \tag{11}$$

This can be rewritten in a form equivalent to the unsteady heat diffusion equation:

$$\rho c\frac{\partial\phi}{\partial t} = \frac{\partial}{\partial x}\left\{k\frac{\partial\phi}{\partial x}\right\} + S \tag{12}$$

The coefficients and source term, S, are non-linear and given by:

$$\rho c = 2R^2\sin^2\phi \tag{13}$$

$$k = R^4\sin^4\phi/C_A \tag{14}$$

$$S = (3C_B R^3/C_A)\cos\phi\sin^2\phi(\partial\phi/\partial x)_t \tag{15}$$

Analysis using the method of characteristics confirms that the equation is parabolic, like the diffusion equation.

Since equations (11) and (12) contain two independent variables (x, t) two boundary conditions are required for solution, namely:

(a) As in the steady state model, the bed depth at the cylinder discharge is equal to the discharge dam height, so (5) remains valid:

$$\phi[0, t] = \phi_0 \tag{16}$$

(b) The volumetric feed rate is given as a function of time, so:

$$Q[L, t] = Q_L[t] \text{ where } t \geq 0 \tag{17}$$

This can be re-stated as a condition on the differential of ϕ by substitution into (4):

$$\left(\frac{\partial\phi}{\partial x}\right)_{t,x=L} = \frac{C_A Q_L[t]}{R^4\sin^4\phi[L,t]} - \frac{C_B}{R\sin\phi[L,t]} \tag{18}$$

The single initial condition required is the axial profile of the bed at $t = 0$, so:

$$\phi[x, t = 0] = \phi_i[x] \text{ where } 0 < x < L \tag{19}$$

In the current study, the dynamic behaviour has been considered for a system initially in the steady state and therefore the initial condition is obtained by solving the steady state flow equation, equation (4), with $Q[L, t]$ equal to its constant value for $t < 0$.

A final comment concerning the approximations involved in deriving the model should be given. For the steady state model of equation (1), it has been assumed that the cylinder slope β and the slope of the bed surface dh/dx, or equivalently $d\phi/dx$, are small. The right-hand-side of (11) is required in its entirety in order to produce the correct steady state model when $\partial\phi/\partial t \rightarrow 0$. However, the right-hand-side of (11) contains terms of both first and second order in the small quantities. It may be that the retention of terms which are second order in the small quantities leads to modifications at that order to (11). The mathematical details of this are an area of continuing investigation; but it will be seen that the model presented here agrees very well with experiment.

Integration of (12) was performed numerically using a marching method in time, with (16) and (17) as boundary conditions at $x = 0$ and $x = L$, and the initial condition described by (19). The numerical method used is based on a discretization method derived from a control-volume formulation as described by Patankar[19].

RESULTS

Experimental measurements are reported of the response of the mass flow rate at the cylinder discharge and the axial bed depth profile following a step change in one of three variables (i) mass feed rate, (ii) rotation speed (iii) axis inclination. Tables on Figures 3–11 give the cylinder axis inclination, mass feed rate and rotation speed. The cylinder geometry and material properties, for the results presented in Figures 3–11, are given in Table 1. On all charts the experimental results are shown as a series of data points and the numerical solution to the model as a solid line. There are no fitted parameters. The experimental measurement of mass flow rate was averaged over the time taken for five cylinder rotations in Figures 3–9, and over a 360 s time interval in Figures 10 and 11. The mean particle residence times calculated from the steady state model are reported for the initial and final steady states. The measurement errors in the bed depth measurement are shown as error bars.

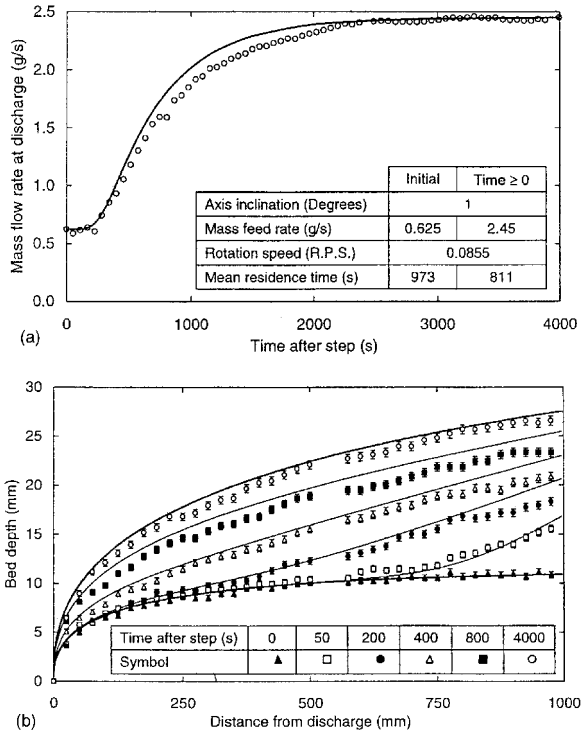

Figure 3. Development of (a) mass flow rate at discharge and (b) axial bed depth profile with time following a step up in the feed rate, Q.

It will be seen from Figures 3–11 that there is good agreement between the experimental measurements and the model. Experimental measurements have also been made for a number of alternative operating points and magnitudes of step in the disturbance variable. In each case the form of the response and level of correlation between model and experiment is equivalent to the results that follow.

Step Up in Feed Rate

The response of the discharge mass flow rate to a large step up in the feed is shown in Figure 3(a). For the first 200 s immediately after the step, the discharge flow rate remains constant at the initial steady level. The discharge rate then begins to increase. The breakthrough time is significantly less than the calculated particle mean residence at both initial and final feed rates. The rate of increase of discharge rate is initially low but grows rapidly. A maximum in the rate of increase of $0.0026\,g\,s^{-2}$ is reached after around 400 s when the discharge rate has reached $1\,g\,s^{-1}$. The rate of increase falls for the remainder of the response, becoming progressively slower after 600 s until the new steady state is reached after around 3000 s.

The development of the axial bed profile during the response is shown in Figure 3(b). A comparison of the profiles for the initial steady state and 50 s following the step shows that in this initial period, material piles up in a region between 0 and 300 mm downstream of the feed; the remainder of the bed is undisturbed. The increase in the depth is greatest at the feed end and decreases in the direction of flow. The profile shape is similar at the next time step, to 200 s, but the bed is now deeper at the feed end and the undisturbed region is restricted to within 100 mm upstream of the discharge. During the next time step up to 400 s, the full bed profile develops and the slope of the bed depth at the discharge increases. The profile after 800 s shows this behaviour to continue. For the remainder of the response, the bed depth continues to increase over the whole length; likewise the slope of bed depth at the discharge increases continuously; the profile eventually converges to the upper steady state concurrently along its whole length. In the final steady state, the bed is deeper and the bed depth slope steeper than in the initial steady state. The time taken for the response to be completed, about 3000 s, is approximately equal to three times the particle residence time (973 s) at the initial steady state feed rate.

The observed discharge response and bed depth profiles can be interpreted using the model: equation (1) shows that the flow rate at a given axial position is dependent on the bed depth and the derivative of the bed depth at that position. The discharge rate remains constant initially because the bed depth profile near the discharge is initially unchanged. The discharge rate subsequently increases as the slope of the bed depth becomes steeper at the discharge.

Step Down in the Feed Rate

The response of the discharge mass flow rate and bed depth profile to a large step down in the feed is shown in Figure 4(a) and (b). The response is qualitatively equivalent to the reverse of the response to a step up in the feed rate shown in Figure 3(a) and (b). Immediately after the step an unexpected fall is observed in the discharge mass flow rate from $2.25\,g\,s^{-1}$ to $2.1\,g\,s^{-1}$. This instantaneous fall is not observed in equivalent experiments in which the feed has been reduced without stopping rotation and it is therefore believed the fall occurs as a result of the experimental procedure.

Table 1. Granular material properties and cylinder geometry for experimental results given in Figures 3–11.

Apparatus	Figures 3 to 8 Cambridge	Figure 9 Birmingham	Figure 10 and 11 Refs 12 and 13
Granular material	Sand	Sand	Ilmenite
Mean particle size mm	0.49	0.49	0.19
Angle of repose Degrees	32	32	27.4
Bulk density $kg\,m^{-3}$	1600	1600	2500
Cylinder radius m	0.0515	0.119	0.0735
Cylinder length m	1	1	5.9
Discharge dam height m	No dam	No dam	0.015

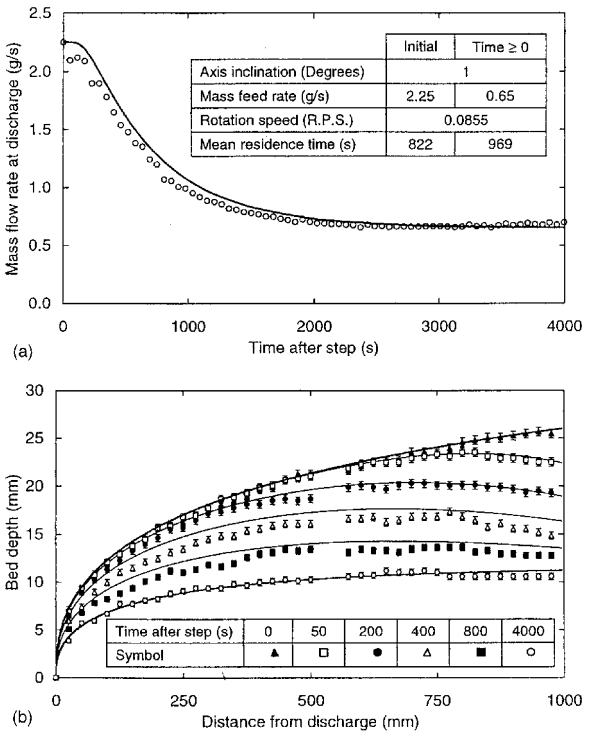

Figure 4. Development of (a) mass flow rate at discharge and (b) axial bed depth profile with time following a step down in the feed rate, Q.

Step Up in the Rotation Speed

The response of the discharge flow rate to a large step up in the rotation speed is shown in Figure 5(a). There is an immediate step up in the discharge rate from $3.1\,g\,s^{-1}$ to $5.8\,g\,s^{-1}$. The discharge rate then remains constant at this upper level for 100 s before beginning to decrease towards the feed rate. The rate of decrease rises rapidly to reach a maximum of $-0.0073\,g\,s^{-2}$ after around 200 s when the discharge rate is $5.4\,g\,s^{-1}$. The rate of decrease falls for the remainder of the experiment becoming progressively slower after 300 s until the discharge rate falls back to equal the feed rate after around 1500 s. The response is completed after four times the particle mean residence time at the higher rotation speed, equivalent to twice the particle mean residence time at the lower rotation speed.

The development of the axial bed depth profile during the response is shown in Figure 5(b). It is qualitatively equivalent to that of the step down in feed rate, Figure 4(b).

The observed discharge response and bed depth profiles can be interpreted using the model: equation (1) shows that the flow rate at any point is proportional to the cylinder rotation speed. Hence, a step up in the discharge rate results from the step up in the rotation speed. Now considering equation (4), it can be seen that the flow rate and rotation speed appear in the same term, $C_A Q$, in the steady state ODE: the initial steady state profile at the low rotation speed could therefore be reproduced at the higher rotation speed by increasing the flow rate. Hence, subsequent to the initial step, the system responds as though it had been subjected to a step down in the feed: Figure 5(a) is similar to Figure 4(a).

Step Down in the Rotation Speed

The response of the discharge flow rate to a large step down in the rotation speed is shown in Figure 6(a). There is an immediate step down in the discharge rate from $3.15\,g\,s^{-1}$ to $1.5\,g\,s^{-1}$. The subsequent response and the development

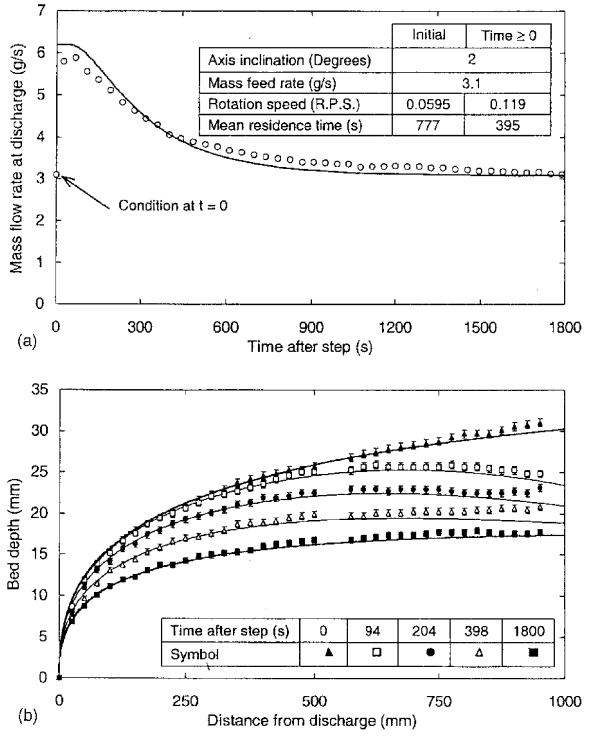

Figure 5. Development of (a) mass flow rate at discharge and (b) axial bed depth profile with time following a step up in the cylinder rotation speed, n.

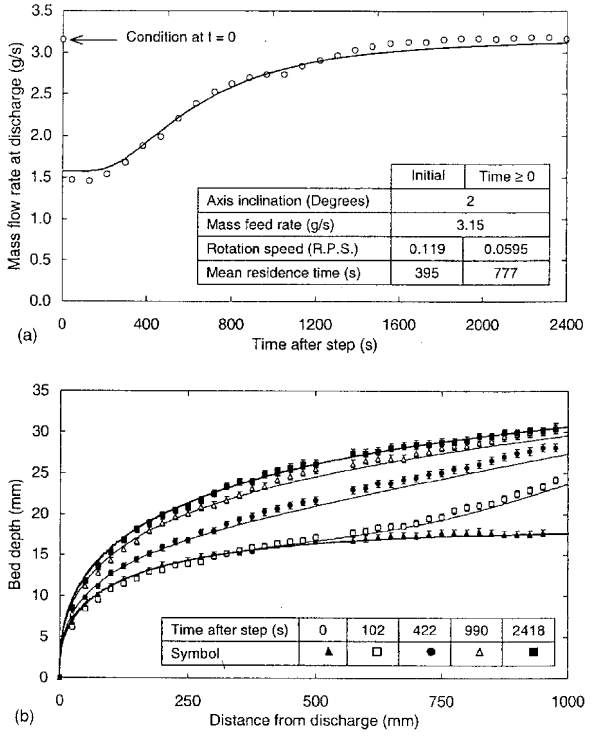

Figure 6. Development of (a) mass flow rate at discharge and (b) axial bed depth profile with time following a step down in the cylinder rotation speed, n.

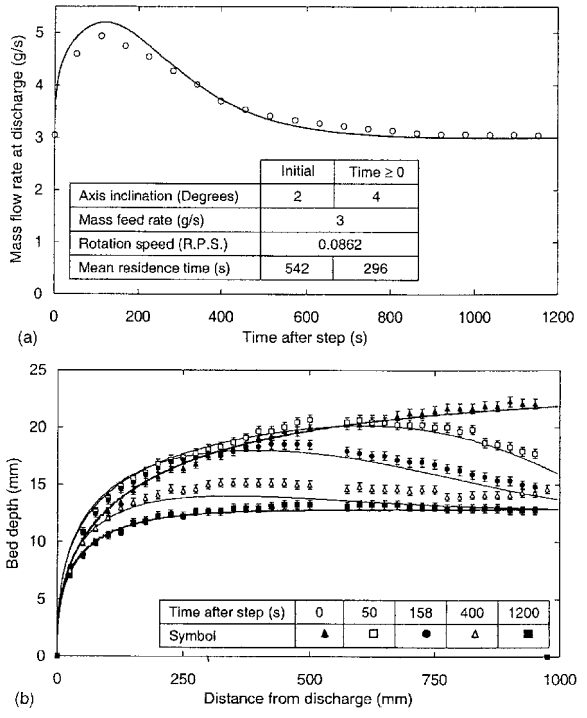

Figure 7. Development of (a) mass flow rate at discharge and (b) axial bed depth profile with time following a step up in the cylinder axis inclination, β.

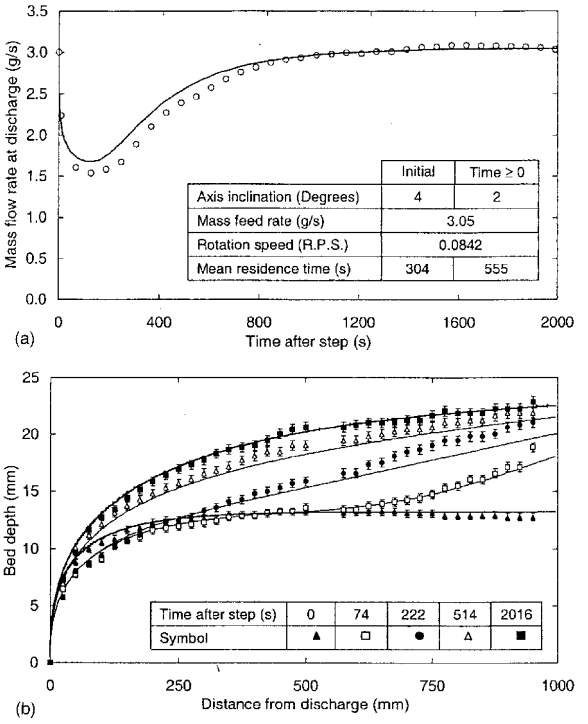

Figure 8. Development of (a) mass flow rate at discharge and (b) axial bed depth profile with time following a step down in the cylinder axis inclination, β.

of the bed depth profile shown in Figure 6(b) are equivalent to those for a step up from $1.5\,g\,s^{-1}$ to $3.15\,g\,s^{-1}$ at the final lower rotation speed.

Step Up in the Axis Inclination

The response of the discharge mass flow rate to a large step up in the axis inclination is shown in Figure 7(a). The discharge flow rate begins to increase immediately after the step. The rate of increase is initially very high but falls rapidly as the discharge rate approaches a maximum of $5\,g\,s^{-1}$ after around 120s. The discharge rate decreases during the remainder of the response. The rate of decrease rises initially to reach a maximum of $-6.7\,g\,s^{-2}$ after around 230 s when the discharge rate is $4.5\,g\,s^{-1}$. The rate of decrease falls for the remainder of the experiment, becoming progressively slower after 400 s until the new steady state is reached after around 1200 s. The response is completed after approximately twice the particle residence time at the initial lower axis inclination, equivalent to four times the particle residence time at the final higher axis inclination.

The development of the bed depth profile during the response is shown in Figure 7(b). As can be seen by comparison of the initial and 50 s profiles there is an immediate response to the step, at all positions in the bed. A turning point, ($dh/dx = 0$) develops in the bed depth profile at an axial distance of 600 mm from the discharge and the bed depth slope at the discharge is increased. The profile crosses the initial profile at an axial distance of 550 mm from the discharge; downstream the depth becomes deeper than the initial level and upstream the depth becomes shallower, falling to a minimum at the feed. The profile at 158 s has a similar shape: the turning point ($dh/dx = 0$) advances in the flow direction to a distance of 400 mm from the discharge and there is a further increase in the discharge bed depth slope. The crossing point with the initial profile advances in the flow direction to a distance of 325 mm from the discharge and upstream there is a further fall in the depth. After 400 s the profile is approaching the final steady state, the turning point has advanced to a distance of 325 mm from the discharge and at all points the bed depth and bed depth slope are below the initial level.

Step Down in the Axis Inclination

The response of the discharge mass flow rate and bed depth profile to a large step down in the axis inclination are shown in Figure 8(a) and (b). The response is qualitatively equivalent to the reverse of the response to a step up in the axis inclination shown in Figure 7(a) and (b). The response is completed after approximately two particle residence times at the final lower axis inclination, equivalent to four particle residence times at the initial higher axis inclination.

Birmingham University Apparatus

The response of the discharge mass flow rate to a step up and step down in the feed rate in the larger diameter Birmingham University cylinder is shown in Figure 9. The form of the response is equivalent to that previously described.

Comparison with Published Work

The model proposed by the current authors is compared with published experimental data in Figures 10 and 11.

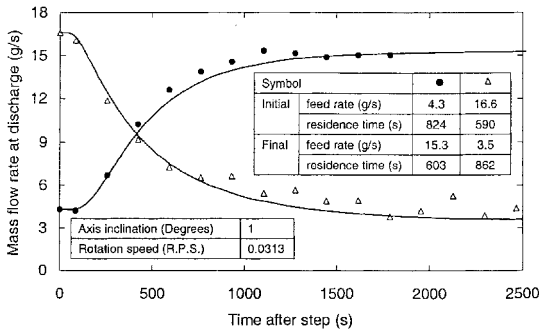

Figure 9. Development of mass flow rate at discharge with time following a step in the feed rate, Q, for a cylinder of diameter 0.238 m.

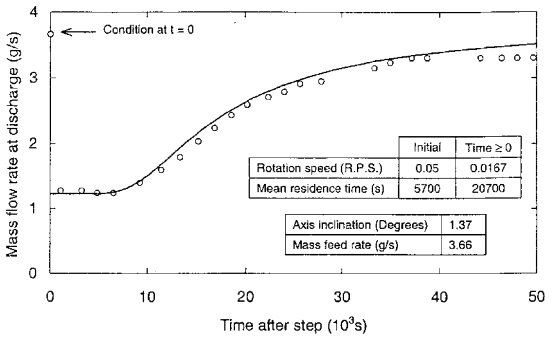

Figure 11. Published experimental data of Sai *et al.*[12]: Development of mass flow rate at discharge with time following a step down in the rotation speed, n.

Figure 10 shows the response of the discharge flow rate to a step change in the feed rate: the experimental data for the step up in feed rate are taken from Figure 9 of Sai *et al.*[12] and for the step down in feed rate from Figure 3 of Sriram and Sai[13]. Figure 11 shows the response of the discharge flow rate to a step down in the rotation speed: the experimental data are taken from Figure 10 of Sai *et al.*[12]. The cylinder geometry and granular material properties are given in Table 1: it can be seen that they are considerably different from those of the authors' experiments. In each case the form of the response is the same as that observed in the current study and there is good quantitative correlation between the model and the experimental data.

CONCLUSIONS

This paper reports the results of an experimental and theoretical study to investigate the transient response of the granular flow through a laboratory scale inclined rotating cylinder to large step changes in one of three variables (i) mass feed rate, (ii) rotation speed, or (iii) axis inclination. Experiments were conducted using sand of mean particle size 490 μm, bulk density 1600 kg m^{-3} and angle of repose 32°, in a cylinder lined on the inner wall with sandpaper. Two cylinders were used, one of length 1 m and diameter 0.103 m, the second of length 1 m and diameter 0.238 m. A number of values of rotation speed and axis inclination were considered within the ranges 0.05–0.125 r.p.s and 1°–3° respectively. Similarly, the granular feed rate was adjusted to produce a total granular bed inventory between 5% and 25% of the cylinder volume. In all cases the transverse motion of the granular bed was in the rolling mode as described by Henein *et al.*[1]. With the system initially in the steady state, the step change was imposed, and the resulting discharge flow rate and bed depth axial profile measured as functions of time.

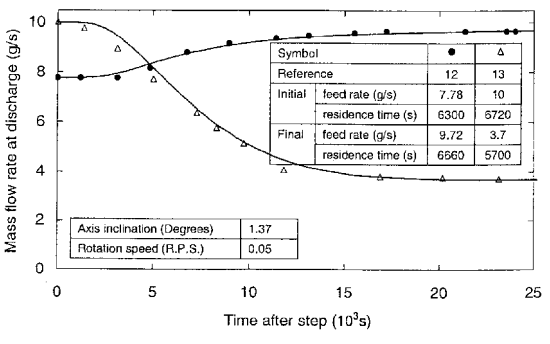

Figure 10. Published experimental data of Sai *et al.*[12], and Sriram and Sai[13]: Development of mass flow rate at discharge with time following a step, up or down, in the feed rate, Q.

A mechanistic model for the transient response has been derived based on the steady state model first proposed by Saeman[11], and Kramers and Croockewit[2]. This gives a non-linear partial differential equation, equivalent to a one dimensional unsteady diffusion equation with variable coefficients. Solution was obtained numerically. The model has no adjustable parameters, making it useful for scale-up.

Good agreement is found between the model and experiment, both in the range of cases considered in the current experiments and also in comparison with the published experimental data of Sriram and Sai[13], and Sai *et al.*[12]. For these published data, the system differs considerably from that in the current study; the cylinder used was of length 5.9 m and diameter 0.147 m and the granular material was ilmenite, mean particle size 190 μm, bulk density 2500 kg m^{-3} and angle of repose 27.4°.

The results to date provide good preliminary evidence that the dynamic model described is applicable for scale-up; however, further investigation is required in three areas:

(a) The length of the cylinder is a critical parameter in the mathematical formulation of the model, therefore an experimental investigation of the transient response in a cylinder of the same diameter but double the current length is under way.

(b) The mechanism of particle motion proposed in the steady state model assumes that particles spend a negligible time falling down the free surface, and therefore from continuity that the thickness of the falling layer is negligible. If the results observed at laboratory scale are to remain valid with scale-up of the cylinder diameter the flow pattern in a transverse section of the granular bed must scale proportionally. To test this assumption, work is under way to investigate the effect of bed depth, rotation speed and cylinder diameter on the transverse flow in the granular bed using the Positron Emission Particle Tracking technique at Birmingham University, as described by Parker *et al.*[18].

(c) Results here given are for sand and ilmenite. The authors expect the theory to apply for other free-flowing materials. But for cohesive materials, e.g. certain food grains, the theory would probably need modification.

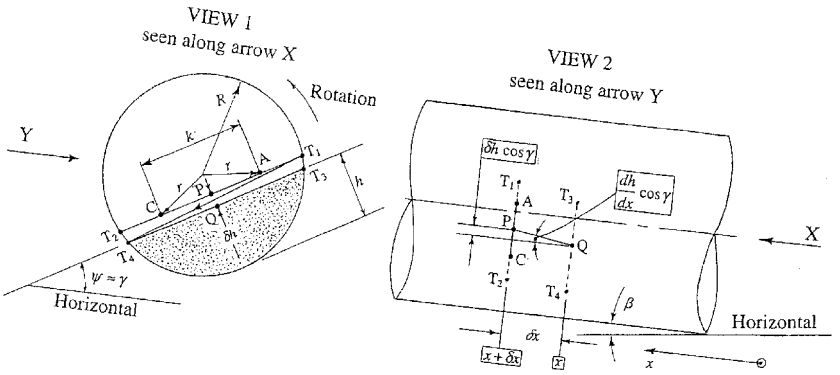

Figure A1. Particle motion in a rotating cylinder containing a granular bed of depth, h, varying along the cylinder; h is independent of time. Cylinder slope β is small, e.g. 3°. The axial movement of an outside particle, falling from T_1 to T_4, is δx.

APPENDIX

The Steady State Equation Governing Bed Depth

For a granular bed in a slowly rotated cylinder operating in the steady state, the bed depth is governed by (1) which is derived from the equation given by Kramers and Croockewit[2], based on the work of Saeman[11]. However, Saeman's[11] analysis is hard to follow. A simple derivation is given below to clarify the assumptions underlying (1), important because they are the basis of this work's unsteady state analysis.

Figure A1 shows the geometry for a small cylinder slope β, of order 1°–5°. At slow rotation speeds, a slumping or rolling bed is formed, and it is assumed the bed surface is flat: in view 1, the bed slope is ψ. For finite β and constant bed depth h, it can be shown that ψ is related to the angle of repose γ by the equation:

$$\cos\gamma = \cos\psi\cos\beta \tag{A1}$$

Using typical values, $\gamma = 30°$, $\beta = 3°$, gives $\psi = 29.86°$; thus, ψ is very close to γ.

Figure A1 shows the geometry when the bed depth h varies with distance x, measured from the discharge end. An element of bed surface is assumed to be flat over the length δx shown in Figure A1, view 2. At position x, the top of the bed is the straight line T_3T_4, Figure A1, view 1; at position $x + \delta x$, the top of the bed is T_1T_2. The line T_1T_4 is a path of steepest descent, the track of an outer particle which has just moved round, in contact with the cylinder wall, from T_2 to T_1.

An inner particle is considered moving round, in $x + \delta x$, from C to A at radius r, Figure A1, view 1. From A, the particle moves down a line of steepest descent which, as it will be shown, is in the plane $T_1T_2T_3T_4$. The line PQ, Figure A1 views 1 and 2, is normal to T_1T_2 and to T_3T_4. In view 1, PQ has length δh; it follows that in view 2, the angle between PQ and the kiln axis is $(\mathrm{d}h/\mathrm{d}x)\cos\gamma$.

Figure A2 shows the geometry of a line of steepest descent AD. The plane ACB contains both the lines T_1T_2 and T_3T_4: thus, from Figure A1, view 2, the angle ABE in Figure A2 is $\beta + (\mathrm{d}h/\mathrm{d}x)\cos\gamma$. The plane $EBDC$, Figure A2, is horizontal: AD is almost, but not quite, the complete flight of the particle; the flight terminates where AD, extrapolated, meets the line through C parallel to AB. But in view of the smallness of angles β and $\mathrm{d}h/\mathrm{d}x$, CD in Figure A2 can be taken as the axial movement of a particle starting from A.

In Figure A2, triangles ADC and BAC are similar, so

$$\frac{CD}{AC} = \frac{s}{k} = \frac{AC}{BC} \approx \frac{k}{BE} \tag{A2}$$

Here it is assumed that $BE \approx BC$, because β is small and hence angle EBC is small.

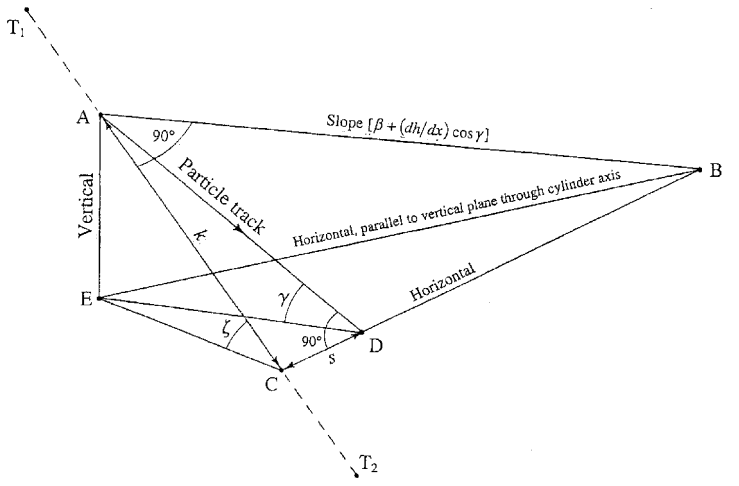

Figure A2. Geometry of surface particle movement for the particle bed of Figure A1.

From triangle *ABE*,

$$BE[\beta + (\mathrm{d}h/\mathrm{d}x)\cos\gamma] = AE = k\sin\zeta \approx k\sin\gamma \quad \text{(A3)}$$

Here it is assumed that the angle ζ, Figure A2, is nearly equal to γ the angle of repose. Referring again to the case when β is finite and h is independent of x, another result is that $\sin\zeta = \sin\psi\cos\beta$; with $\gamma = 30^\circ$, $\beta = 3^\circ$; (A1) is used to get $\zeta = 29.82^\circ$, thus, $\zeta \approx \gamma$ is a good approximation.

Eliminating k/BE from equations (A2) and (A3), and replacing β by $\tan\beta$, gives

$$\frac{s}{k} = \frac{\tan\beta}{\sin\gamma} + \frac{\mathrm{d}h}{\mathrm{d}x}\cot\gamma \quad \text{(A4)}$$

This equation was given by Kramers and Croockewit[2] but with x measured in the opposite direction. The equation shows that s/k is independent of k, so all particle tracks have the same s/k and the tracks must therefore all lie in the plane $T_1T_2T_3T_4$, Figure A1, as proposed above.

The final step in deriving equation (1) is to assume that:

(a) In Figure A2, the flight time from *A* to *D* is negligible;
(b) The residence time in the cylinder is due to the time taken to move over arcs of radius *r*, Figure A1, from *C* to *A*.

By integrating over the cross-section of the granular bed, Figure A1, using (A4), the granular flow rate can be related to h by:

$$Q = \frac{4\pi nR^3}{3}\left(\frac{\tan\beta}{\sin\gamma} + \frac{\mathrm{d}h}{\mathrm{d}x}\cot\gamma\right)\left(2\frac{h}{R} - \left(\frac{h}{R}\right)^2\right)^{3/2} \quad \text{(A5)}$$

given by Kramers and Croockewit[2]. Equation (A5) is readily transformed into (1) using $h = R(1 - \cos\phi)$.

NOMENCLATURE

A	area of the material bed in a plane perpendicular to the cylinder axis, m^2
C_A	coefficient defined in equation (2), s
C_B	coefficient defined in equation (3)
g	acceleration of gravity, $m\,s^{-2}$
h	height of the bed above the cylinder wall measured perpendicular to the bed surface, m
k	coefficient in equation (12), defined in equation (14), $m^4\,s^{-1}$
L	cylinder length, m
n	cylinder rotation speed, $rev\,s^{-1}$
Q	volumetric flow rate of granular material, $m^3\,s^{-1}$
Q_L	volumetric feed rate of granular material, $m^3\,s^{-1}$
R	cylinder radius, m
S	source term in equation (12), defined in equation (15), $m^2\,s^{-1}$
t	time, s
x	axial distance from cylinder discharge end, m

Greek symbols

β	inclination of cylinder axis to horizontal, rad
ϕ	maximum half angle subtended by the bed at the cylinder axis, rad subscript *0* : cylinder discharge end. Subscript *i* : Initial profile
γ	static angle of repose of the bed material, rad
ρ c	variable coefficient in equation (12), defined in equation (13), m^2

REFERENCES

1. Henein, H., Watkinson, A.P. and Brimacombe, J.K., 1983, Experimental study of transverse bed motion in rotary kilns, *Metallurgical Trans B*, 14B: 191.
2. Kramers, H. and Croockewit, P., 1952, The passage of granular solids through inclined rotary kilns, *Chem Eng Sci*, 1: 259.
3. Lebas, E., Houzelot, J.L., Ablitzer, D. and Hanrot, F., 1995, Experimental study of residence time, particle movement and bed depth profile in rotary kilns, *Canad J Chem Eng*, 73: 173.
4. Vahl, L. and Kingma, W.G., 1952, Transport of solids through horizontal rotary cylinders, *Chem Eng Sci*, 1: 253.
5. Abouzeid, A.Z.M. and Fuerstenau, D.W., 1980, A study of the hold-up in rotary drums with discharge end constrictions, *Powder Technol*, 25: 21.
6. Chaterjee, A., Mukhopadhyay, P.K., Srivastava, M.P and Sathe, A.V., 1983, Flow of materials in rotary kilns used for sponge iron manufacture: Part 1. Effect of some operational variables, *Metallurgical Trans B*, 14B: 375.
7. Chatterjee, A., Mukhopadhyay, P.K. and Sathe, A.V., 1983, Flow of materials in rotary kilns used for sponge iron manufacture: Part 2. Effects of kiln geometry, *Metallurgical Trans B*, 14B: 383.
8. Hogg, R., Austin, L.G. and Shoji, K., 1974, Axial transport of dry powders in horizontal rotating cylinders, *Powder Technol*, 9: 99.
9. Sai, P.S.T., Sankaran, K., Philip, Z.G., Suresh, V., Damodaran, A.D. and Surender, G.D., 1990, Residence time distribution and material flow studies in a rotary kiln, *Metallurgical Trans B*, 21B: 1990.
10. Chaterjee, A. and Mukhopadhyay, P.K., 1983, Flow of materials in rotary kilns used for sponge iron manufacture: Part 3. Effect of ring formation within the kiln, *Metallurgical Trans B*, 14B: 393.
11. Saeman, W.C., 1951, Passage of solids through rotary kilns: factors affecting time of passage, *Chem Eng Prog*, 47: 508.
12. Sai, P.S.T., Surender, G.D. and Damodaran, A.D., 1992, Prediction of axial velocity profiles and solids hold-up in a rotary kiln, *Canad J Chem Eng*, 70: 438.
13. Sriram, V. and Sai, P.S.T., 1999, Transient response of granular bed motion in rotary kiln, *Canad J Chem Eng*, 77: 597.
14. Perron, J. and Bui, R.T., 1994, Fours rotatifs: Modele dynamique du mouvement du lit, *Canad J Chem Eng*, 72: 16.
15. des Boscs, J., 1998, Granular motion in rotating drums, *MPhil Thesis* (submitted to the Faculty of Engineering of The University of Birmingham).
16. Boateng, A.A. and Barr, P.V., 1997, Granular flow behaviour in the transverse plane of a partially filled rotating cylinder, *J Fluid Mech*, 330: 233.
17. Nakagawa, M., Jeong, E.K., Fukushima, E., Caprihan, A. and Altobelli, S.A., 1993, Non-invasive measurement of granular flows by magnetic resonance imaging, *Experiments in Fluids*, 60: 54.
18. Parker, D.J., Seville, J.P.K., Martin, T.W. and Dijkstra, A.E., 1997, Positron emission particle tracking studies of spherical particle motion in rotating drums, *Chem Eng Sci*, 52: 2011.
19. Patankar, S.V., 1980, *Numerical Heat Transfer and Fluid Flow* (Hemisphere Publishing Corporation).

ACKNOWLEDGEMENTS

We thank the EPSRC and ICI for a CASE award for RJS, and the EPSRC for support through grant GR/M23083. We thank Huntsman Tioxide, Billingham and the PEPT group at the University of Birmingham (Jonathan Seville, David Parker and Robin Forster) for their help and advice.

ADDRESS

Correspondence concerning this paper should be addressed to Professor J. F. Davidson, Department of Chemical Engineering, University of Cambridge, Pembroke St, Cambridge, CB2 3RA, UK. E-mail: david_scott@cheng.cam.ac.uk

The manuscript was received 16 May 2000 and accepted for publication after revision 21 September 2000.